Lithos 120 (2010) 1–13

Contents lists available at ScienceDirect

Lithos

journal homepage: www.elsevier.com/locate/lithos

The continental lithosphere–asthenosphere boundary: Can we sample it?

Suzanne Y. O'Reilly *, W.L. Griffin

GEMOC ARC National Key Centre, Department of Earth and Planetary Sciences, Macquarie University, Sydney, NSW 2109, Australia

ARTICLE INFO

Article history:
Received 29 July 2009
Accepted 20 March 2010
Available online 31 March 2010

Keywords:
Lithosphere–asthenosphere boundary
Lithosphere evolution
Cratonic lithosphere
Archean lithosphere
Asthenosphere composition
Subcontinental lithospheric mantle

ABSTRACT

The lithosphere–asthenosphere boundary (LAB) represents the base of the Earth's lithosphere, the rigid and relatively cool outer shell characterised by a conductive thermal regime, isolated from the convecting asthenosphere. Chemically, the LAB should divide a lithospheric mantle that is variably depleted in basaltic components from a more fertile asthenosphere. In xenolith suites from cratonic areas, the bottom of the depleted lithosphere is marked by a rapid downward increase in elements such as Fe, Ca, Al, Ti, Zr and Y, and a rapid decrease in the median Mg# of olivine, reflecting the infiltration of mafic melts and related fluids. Eclogites and related mafic and carbonatitic crystallisation products are concentrated at the same depths as the maximum degrees of metasomatism, and may represent the melts responsible for this refertilisation of the lithosphere. This refertilised zone, at depths of ca 170–220 km beneath Archean and Proterozoic cratons, is unlikely to represent a true LAB. Re–Os isotopic studies of the deepest fertile peridotite xenoliths show that they retain evidence of ancient depletion events; seismic tomography data show high-velocity material extending to much greater depths beneath cratons. The cratonic "LAB" probably represents a level where asthenospheric melts have ponded and refertilised the lithosphere, rather than marking a transition to the convecting asthenosphere. Our only deeper samples are rare diamond inclusions and some xenoliths inverted from majoritic garnet, which are unlikely to represent the bulk composition of the asthenosphere. In younger continental regions the lithosphere–asthenosphere boundary is shallower (commonly at about 80–100 km). In regions of extension and lithosphere thinning (e.g. eastern China, eastern Australia, Mongolia), upwelling asthenosphere may cool to form the lowermost lithosphere, and may be represented by xenoliths of fertile garnet peridotites in alkali basalts.

The LAB is a movable boundary. It may become shallower due to thermal and chemical erosion of the lithosphere, assisted by extension. Refertilised lithospheric sections, especially where peridotites are intermixed with eclogite, may be capable of gravitational delamination. The lithosphere–asthenosphere boundary may also be deepened by subcretion of upwelling hot mantle (e.g. plumes). This process may be recorded in the strongly layered lithospheric mantle sections seen in the Slave Craton (Canada), northern Michigan (USA) and the Gawler Craton (Australia).

© 2010 Elsevier B.V. All rights reserved.

1. Introduction

The lithosphere–asthenosphere boundary (LAB) beneath the continents is a surface of first-order importance in understanding the geochemical and geodynamic evolution of our planet. It coincides with the lower limit of the subcontinental lithospheric mantle (SCLM), so its identification depends on understanding the nature (composition, architecture, origin and evolution) of the SCLM.

The subcontinental lithospheric mantle (SCLM) is easily defined, at least in concept: it is the non-convecting uppermost part of the mantle lying beneath a volume of continental crust. It forms the lowermost part of the lithospheric plate complex that moves in a relatively rigid way over the hotter and rheologically weaker asthenosphere. Lithosphere is non-convecting and thus is characterised by conductive geotherms, though magmatic activity may locally produce a temporary advective geotherm (O'Reilly and Griffin, 1985). The intersection of the conductive geotherm with the fluid-saturated solidus of peridotite may mark the division of the lithosphere into an upper mechanical boundary layer and a lower thermal boundary layer, which though weaker, still sustains a conductive geotherm (e.g. McKenzie and Bickle, 1988). The actual lithosphere/asthenosphere interface occurs at the intersection of the conductive geotherm with the asthenosphere adiabat at the mantle potential temperature of about 1300 °C.

The *composition* of the SCLM, as reflected in mantle-derived xenoliths and exposed massifs, is complex; it reflects an original depletion in basaltic components (to high degrees beneath cratons, and to lesser degrees beneath younger crust), and subsequent geochemical overprinting (refertilisation) by multiple episodes of melt and fluid infiltration. Beneath cratonic areas the SCLM is generally thick (150–250 km) and refractory (i.e. high in Mg and low in Ca, Al); beneath younger mobile belts

* Corresponding author.
E-mail address: sue.oreilly@mq.edu.au (S.Y. O'Reilly).

0024-4937/$ – see front matter © 2010 Elsevier B.V. All rights reserved.
doi:10.1016/j.lithos.2010.03.016

and extensional areas it typically is thinner and compositionally more "fertile" (i.e. lower in Mg and richer in Ca, Al, Fe, Ti and other "basaltic" components).

The *origin* of the SCLM, and particularly ancient *cratonic* SCLM, is more controversial, but critical to meaningful geodynamic modeling. As summarised by O'Reilly and Griffin (2006), it may have formed as residues from high-degree partial melting (see Griffin et al., 2009a, references therein; Pearson and Wittig, 2008), by accretion of plume heads to pre-existing lithosphere (e.g. Kaminsky and Jaupart, 2000), or by the subcretion of subducting plates ("subduction stacking"; Helmstedt and Gurney, 1995; for a dissenting view see Griffin and O'Reilly, 2007a,b). Recent work (Griffin et al., 2009a; Afonso et al., 2008) suggests that most of the preserved Archean lithospheric mantle was formed by processes distinct from those forming younger lithospheric mantle, and that the original Archean lithospheric mantle was much more refractory (depleted in Fe, Al, Ca and other basaltic components) than traditional estimates of its composition based on xenolith data (e.g. Boyd, 1989; Boyd et al., 1999; and review in Griffin et al., 1999a,b,c). The volume of lithosphere formed in the Archean was much greater than previously estimated and most of it may have stabilised by about 3 Ga ago (Griffin and O'Reilly, 2007b; Begg et al., 2009; Griffin et al., 2009a; O'Reilly et al., 2009).

Younger SCLM has formed by different processes, dominated by cooling and underplating of upwelling asthenosphere. This can be induced by delamination of older lithosphere (e.g. beneath the East Asia Orogenic Belt; Zheng et al., 2006a), by widespread extension related to subduction rollback (e.g. north-eastern China, Griffin et al., 1998b; Zheng et al., 2005, 2007; Yang et al., 2008; references therein), or by full-fledged rifting resulting in the formation of ocean basins. Geochemical evidence and seismic tomography for thinned lithospheric regions and ocean basins reveal that domains with high seismic velocity probably represent remnants of ancient lithospheric mantle stranded beneath younger terranes and within oceanic basins (e.g. O'Reilly et al., 2009).

The upper limit of the SCLM is the crust–mantle boundary, which may or may not correspond to the seismically defined Mohorovicic discontinuity (*Moho*; see Griffin and O'Reilly, 1987). The base of the depleted SCLM can be recognized in xenolith suites, and in some areas by geophysical methods (Jones et al., 2010-this volume; references therein). This horizon, which typically corresponds to temperatures of about 1300 °C, is commonly described as the "Lithosphere–Asthenosphere boundary." But does it really represent a transition from stable lithosphere to convecting asthenosphere? Do we have any samples that might represent the asthenosphere? In this paper we review some of the petrological and geochemical evidence for the nature of this "LAB" beneath both cratons and younger areas, to answer these questions.

2. The cratonic LAB

2.1. Xenolith-based geotherms – the enabling technology

The use of geotherms constructed using temperature (T) and pressure (P) data calculated from the compositions of coexisting minerals in xenoliths was a major breakthrough in mantle petrology. It allowed lithospheric mantle rock types to be put into a spatial context, thus providing a basis for defining the rock-type distribution and the structure (including the lower boundary) of the lithospheric mantle. This advance was initiated by early experimental high T and P simulations of a range of mantle mineral assemblages (e.g. Boyd, 1970; MacGregor, 1974; Wood and Banno, 1973). The presence of coexisting garnet, clinopyroxene, orthopyroxene and olivine (a garnet lherzolite assemblage) in mantle xenoliths enables the calculation of their P and T of equilibration: data for a series of such xenoliths over a significant depth range delineates the geotherm for that timeslice and that mantle section. This empirical methodology overcomes the problems associated with model geotherm calculations that use extrapolated heat flow measurements and require assumptions about deep crustal heat production and conductivity. Once a xenolith geotherm has been established for a given time and place, then other xenolith rock types, for which only T can be calculated from the mineral assemblage (e.g. eclogites and spinel peridotites) can be assigned a depth of origin by reference of their T to the established geotherm. Early xenolith geotherms encountered considerable skepticism about their significance. Some workers (e.g Harte and Freer, 1982) argued that such P–T arrays merely represent sliding closure temperatures for various mineral equilibria and thus carry no real information about geothermal gradients.

However, the empirical xenolith geotherms have stood the test of time, following rigorous applications to numerous xenolith suites and their lithospheric sections, supplemented by continuing experimental validation of mantle assemblages and their physical conditions of formation (e.g. Brey et al., 1990; Brey and Kohler, 1990; Kohler and Brey, 1990). The first geotherms were established for cratonic regions where garnet–lherzolite assemblages are relatively common, and the relatively cool geotherms for cratonic regions became generally accepted as an accurate reflection of the thermal regime in these tectonic environments.

The first off-craton xenolith-based geotherms were constructed for Tanzania (Jones et al., 1983) and eastern Australia (Griffin et al., 1984; O'Reilly and Griffin, 1985). These studies showed that geotherms in young tectonic regions with basaltic activity are similar worldwide (the "basaltic province" geotherm). These geotherms, before thermal relaxation to steady-state conditions, are both high and strongly curved due to advective heat transfer from the passage of basaltic magmas, and the ponding of magmas around the crust–mantle boundary (Griffin and O'Reilly, 1987; O'Reilly et al., 1988). The concept that there are many types of geothermal gradients was originally controversial as the commonly accepted wisdom was that there were two geothermal gradient regimes, one representing "continental" (=cratonic) domains and the other found in oceanic settings. O'Reilly (1989) and O'Reilly and Griffin (1996) summarised the variety of geotherms found in different tectonic environments, and it is now widely accepted that geothermal gradients are indeed variable and reflect a range of tectonic processes.

2.2. Kinked geotherms and sheared xenoliths — the history of an idea

Boyd and Nixon (1975) published one of the first xenolith-based paleogeotherms, applying new experimental calibrations of pyroxene–garnet thermobarometry to a suite of xenoliths from the Thaba Putsoa kimberlite in Lesotho. They demonstrated that xenoliths with granular, equilibrated microstructures lay along a model conductive geotherm (Pollack and Chapman, 1977) corresponding to a typical cratonic surface heat flow of ca 40 mW/m^2, and extending to $T \approx 1100$ °C. Lherzolitic xenoliths with fluidal porphyroclastic ("sheared") microstructures gave higher T, up to ≥ 1400 °C, but over a narrow range of pressures, placing them above the conductive geotherm (Fig. 1). This "kinked" geotherm, associated with evidence of strong shearing in the higher-T xenoliths, led to the suggestion that the sheared lherzolites represent samples of the convecting asthenosphere.

This idea became even more attractive when Mercier (1979) used experimental and theoretical annealing experiments to demonstrate that the microstructures of the sheared xenoliths could not be preserved for more than a few years at the temperatures recorded by their mineral chemistry. This required that the shearing was essentially contemporaneous with entrainment of the xenoliths in the kimberlite (also see Gregoire et al., 2006). Chemical analyses showed that the sheared xenoliths are highly fertile in terms of basaltic components (Mg# (Mg/(Mg + Fe)) ≤ 91, high Ca, Al, and Ti); their bulk compositions approximate estimates of the Primitive Upper

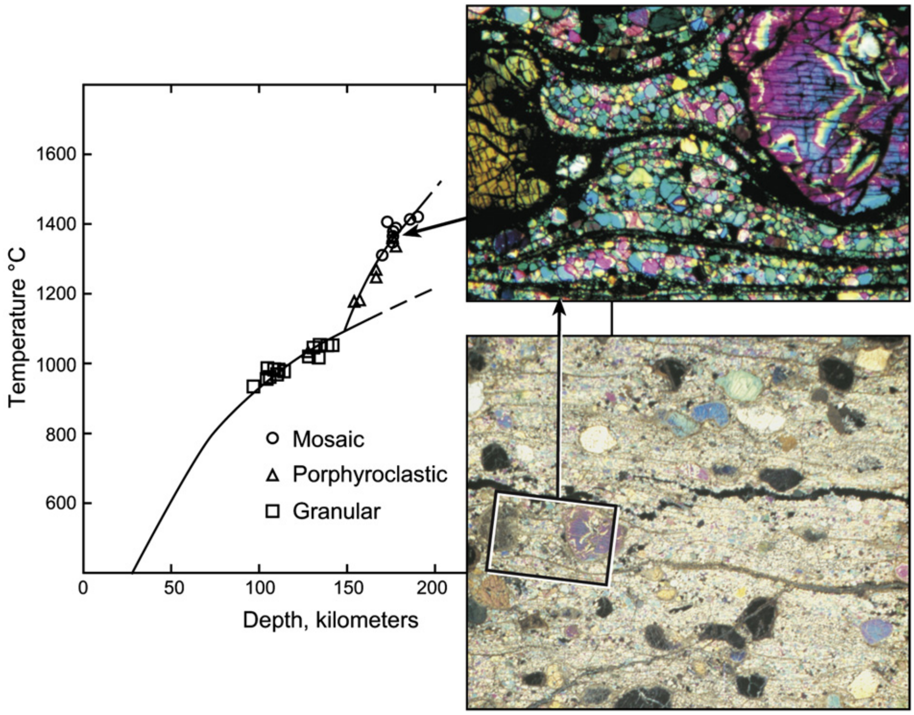

Fig. 1. The original N. Lesotho xenolith geotherm of Boyd and Nixon (1975) showing the conductive low-*T* limb defined by garnet lherzolites with equilibrated granular microstructures, and the "kinked" limb defined by high-*T* sheared peridotites such as PHN1611 (photomicrographs). Base of upper photomicrograph is 0.5 mm long.

Mantle (or "Pyrolite"), in contrast to the refractory compositions of the lower-*T* granular peridotites. The sheared lherzolites also have chondritic REE patterns and depleted isotopic signatures (i.e. high $^{143}Nd/^{144}Nd$, low $^{87}Sr/^{86}Sr$). All these lines of evidence supported the idea that the sheared lherzolite xenoliths might actually be samples of the convecting asthenosphere (Boyd, 1987).

This interpretation began to be less plausible as more detailed data emerged, especially with studies of zoning in the minerals of the sheared lherzolites (Smith and Boyd, 1987; Smith et al., 1991, 1993; Griffin et al., 1996). The garnet porphyroblasts in particular are strongly zoned, with rims depleted in Cr and enriched in Fe, Ti, Y and Zr relative to the cores (Fig. 2A). The trace-element zoning can be modeled in terms of an instantaneous overgrowth, followed by annealing and diffusion to blur the boundary; time scales derived using different estimates of diffusion rates at $T = 1200$ °C range from a few days to hundreds of years (Fig. 2B; Griffin et al., 1996). Smith and Boyd (1987) derived similar estimates from the chemical gradients between Fe-rich and Fe-poor domains in a strongly sheared xenolith.

These studies suggested that the rims of the garnets reflect the addition of Fe, Al, Ca and a range of trace-elements to a protolith that strongly resembled the low-*T* granular garnet lherzolite xenoliths. Estimates of the relative volumes of rims and cores implied that at least 50% of the garnet had been added by this process; correlations between the modal abundance of garnet and clinopyroxene in sheared lherzolites (Fig. 2; Boyd, 1987) would indicate that at least 50% of the clinopyroxene also had been added. The metasomatic addition of so much Ca, Al, Fe, Ti and Na to the originally depleted protolith strongly suggests that the shearing was accompanied by the infiltration of mafic melts. This interpretation of the sheared lherzolites as metasomatised lithosphere, rather than asthenosphere, was corroborated by Re–Os isotopic analyses of whole-rock samples and individual grains of sulfide minerals, which gave model ages (minimum ages of melt depletion) ranging up to 3.5 Ga for some sheared peridotite xenoliths (Walker et al., 1989; Pearson et al., 1995; Griffin et al., 2004b).

The high temperatures recorded by sheared, fertile lherzolites in cratonic situations suggest a thermal perturbation, consistent with the intrusion of mafic melts. The "kinked geotherm" has been the subject of much debate, centred on whether it is an artefact of the methods used to derive *P* and *T* estimates. Finnerty and Boyd (1987) demonstrated that the "kink" (or in some cases a "step") is found in xenolith suites from many cratonic localities worldwide, and is closely correlated with the presence of sheared peridotites. They also showed that it is robust with regard to the choice of different geothermometer–geobarometer pairs available in 1987; Franz et al. (1996) showed that similar results are obtained with a later generation of geothermobarometers (Brey et al., 1990; Brey and Kohler, 1990; Kohler and Brey, 1990). A recent recalibration (Brey et al., 2008) of the gnt–opx barometer yields pressures somewhat lower than earlier calibrations; the difference is greatest for the high-*T* peridotites, an effect that enhances the "kink".

Consideration of the thermal regime at the LAB (Fig. 3) suggests that a "kinked" or "stepped" geotherm is an almost inevitable consequence of a thermal perturbation. In a mantle column at thermal equilibrium, the conductive part of the geotherm (at shallower depths) should merge into the adiabat characteristic of a convecting asthenosphere. A heating event, involving upwelling mantle and melts generated at temperatures above the adiabat, would produce a "kinked" limb connecting the conductive limb and the imposed temperature at the LAB. As heating continues, the "kinked" limb of the array will move up through the lithosphere; its slope will depend on several factors, including the rate of heating. Heat could be supplied by the passage of magmas, but the most efficient mechanism might be the intrusion and crystallization of magmas, releasing latent heat. Such a step in the geotherm is seen within the Slave Craton at about 150 km and 900 °C (Griffin et al., 1999a) with a higher geotherm in the lower part of this SCLM.

2.3. Metasomatism at the "LAB" — data from garnet xenocrysts

Good xenolith suites are relatively rare, and the amount of information on the chemical structure of the SCLM has been increased significantly by the introduction of chemical tomography techniques (see review by O'Reilly and Griffin, 2006), which use xenocryst minerals in mantle-derived magmas to map the vertical distribution of different chemical "process fingerprints". The technique relies on the use of the Ni-in-garnet thermometer (Griffin et al., 1989), which provides a

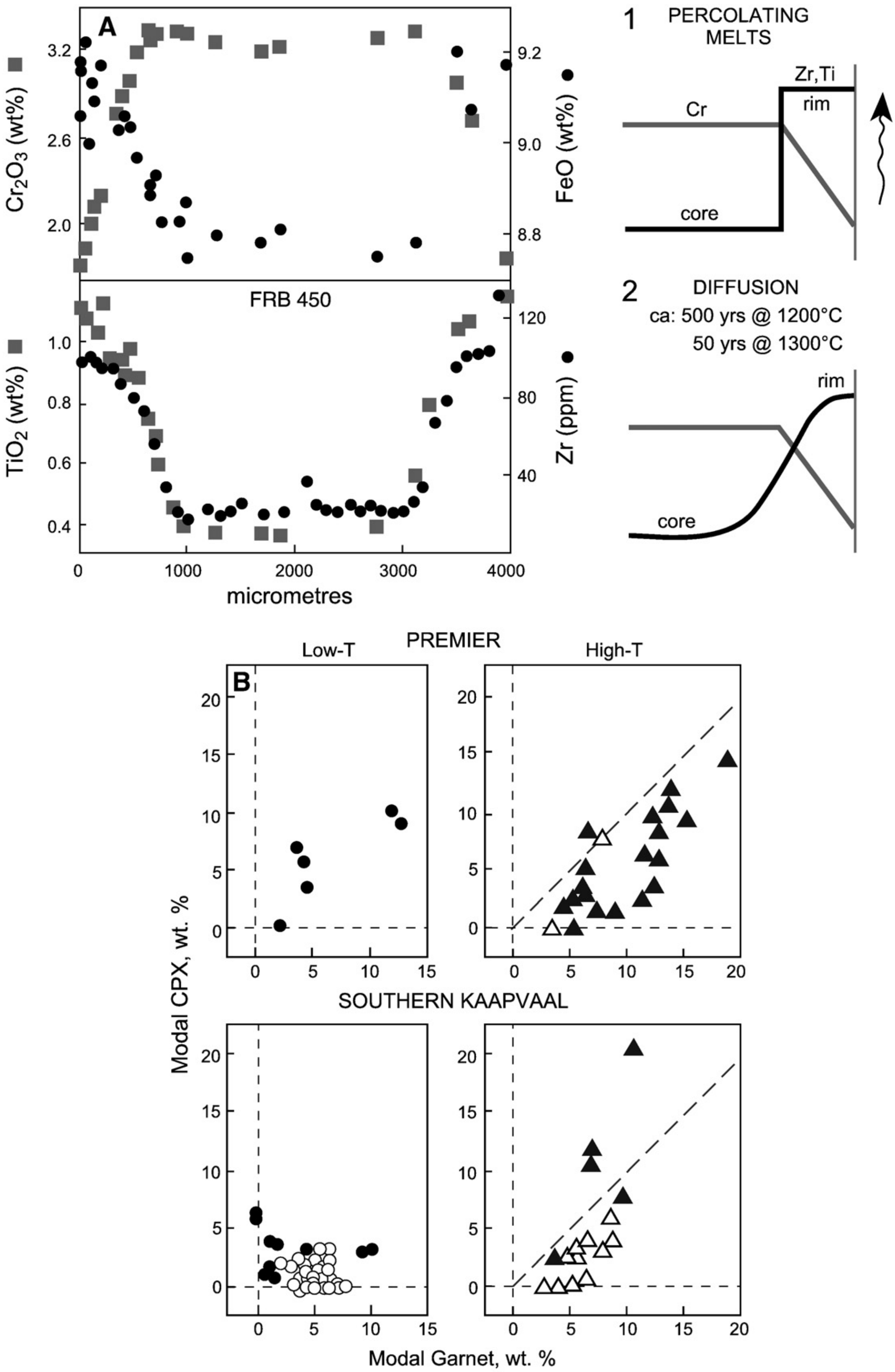

Fig. 2. Refertilisation of sheared lherzolite xenoliths. (A) Zoning of major- and trace-elements in a garnet porphyroblast from xenolith FRB450, and schematic model of an overgrowth followed by diffusion; (B) modal proportions of garnet and clinopyroxene in low- and high-*T* xenoliths from the Premier (Cullinan) Mine and kimberlites of the Kimberley area, South Africa.

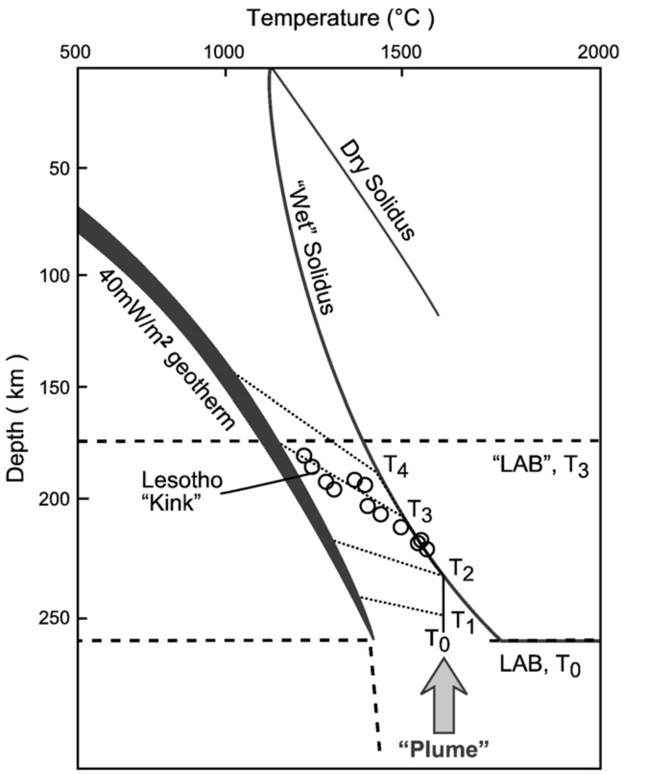

Fig. 3. Development of a kinked geotherm by impingement of a thermal pulse on the base of the lithosphere; the accompanying refertilisation front moves up through the lithosphere to establish a new "LAB" and a (temporarily) kinked geotherm.

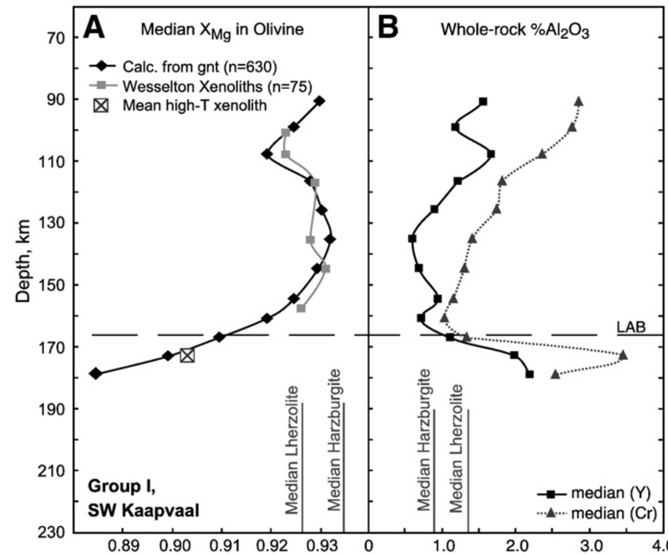

Fig. 4. Geochemical parameters that can be derived from the compositions of xenocrystic peridotitic garnets. (A) X_{Mg} of coexisting olivine vs depth (Gaul et al., 2000) derived from garnets in Group I kimberlites of the SW Kaapvaal craton; the curve derived from garnet data mimics one derived from a large suite of garnet lherzolites and harzburgites. (B) Median whole-rock Al_2O_3 contents vs depth in the same kimberlites, using equations derived from Y and Cr contents of peridotitic garnets (Griffin et al., 1999b).

T estimate for each grain of peridotitic garnet; a depth is assigned to each grain by projection of this *T* to a local geotherm. The geotherm also can be derived from garnet analyses alone (Ryan et al., 1996); this approach gives empirical paleogeotherms that replicate those derived from xenoliths in the same kimberlite. An alternative experimental calibration of the Ni-in-garnet geothermometer (Canil, 1994, 1999) will give higher *T* for low-Ni samples, and lower *T* for high-Ni samples, and does not reproduce the temperatures derived by other experimentally calibrated geothermometers (Griffin et al., 1996), making comparison with xenolith-based geotherms difficult.

Among the useful process fingerprints that can be mapped by this technique is the X_{Mg} of the olivine that coexisted with each garnet grain before it was entrained in the kimberlite (Gaul et al., 2000). There is a close correspondence between the patterns of median X_{Mg} vs depth derived from garnet concentrates and from xenolith suites in the same kimberlite. Fig. 4A shows data from several Group 1 kimberlites in the SW Kaapvaal craton; median X_{Mg} is generally high ($\geq$0.92) at depths less than ca 160 km, then decreases rapidly with depth, to values even lower than the mean high-*T* sheared lherzolite. A local decrease in X_{Mg} (in both the garnet and the xenolith data) around 90–110 km correlates with the widespread development of MARID-type metasomatism at this level of the mantle (Gregoire et al., 2002). The choice of a "LAB" (defined by the depth limit of depleted rocks) depends on the choice of a value of X_{Mg} for the "asthenosphere"; a choice of $X_{Mg}=0.91$ gives a depth of 170 km. Application of this technique to the SCLM beneath different Archean cratons (Fig. 5A) shows a range of patterns. There typically is little overall variation in median X_{Mg} in the upper parts of the sections; all are between $X_{Mg}=0.925$ to 0.935. The transition to lower values is gradual in some sections (e.g. Limpopo Belt) and abrupt in others (e.g. Kroonstadt (S. Africa)); the depth of the "LAB" ranges from ca 175 km to >210 km but the zone of Fe enrichment corresponding to the "LAB" may spread over tens of km vertically in some locations.

Beneath Proterozoic cratons (many of which represent reworked Archean cratons; Begg et al., 2009), the patterns of X_{Mg} vs depth are broadly similar (Fig. 5B). The upper parts of the sections are marginally less magnesian ($X_{Mg}=0.92$–0.93) than beneath Archean cratons, and the degree of Fe enrichment at the base of the depleted sections is generally higher. The transitions may be very sharp (e.g. N. Botswana) or gradual and complex (e.g. Birekte, Guinea); the depth of the "LAB" ranges from 140 to 180 km, and the corresponding zone of Fe enrichment again may spread over tens of km.

A second useful measure of fertility, and thus of depletion and metasomatic re-enrichment, is the whole-rock Al_2O_3 content of peridotites; this parameter can be derived from correlations between whole-rock compositions of peridotite xenoliths and the Y (or Cr) contents of their garnets (Griffin et al., 1998a). A plot of whole-rock Al_2O_3 vs depth for the Group 1 kimberlites of the SW Kaapvaal (Fig. 4B) mirrors the X_{Mg}-depth section; low X_{Mg} correlates with high whole-rock Al_2O_3. This is encouraging, since the two parameters are derived independently. The increase in whole-rock Al_2O_3 at the base of the depleted section appears to be even sharper than the decrease in X_{Mg}. The median whole-rock Al_2O_3 derived from the Y contents of garnets appears to provide a better match to known xenolith compositions than the curve derived from Cr contents of garnets, though the mean difference is only 0.5 wt.%.

In Fig. 6 curves for X_{Mg} and whole-rock Al_2O_3 are combined with chemical tomography sections (O'Reilly and Griffin, 2006) that show the depth distribution of garnets with different signatures of depletion or metasomatism, based on the Y–Zr–Ti–Cr contents of peridotitic garnets. In the upper parts of these sections (<ca 140 km), metasomatic signatures correspond to increases in median whole-rock Al_2O_3, but not to decreases in X_{Mg}. This is consistent with the observation (Griffin et al., 2003a,b) that shallow, phlogopite-rich garnet lherzolites commonly have magnesian olivine. In each of these sections, the base of the depleted part of the SCLM is marked by rapid drops in X_{Mg}, and rises in whole-rock Al_2O_3, with increasing depth. This combination of effects correlates with a dominance of garnets carrying the signature of intense melt-related metasomatism (high Ti, Y, and Zr) as seen in the sheared lherzolites (Fig. 2).

The correlation between X_{Mg}^{oliv}, whole-rock Al_2O_3 and the melt-metasomatism in these mantle sections has been seen in all cratonic areas that we have investigated (Fig. 6). It strongly implies that the

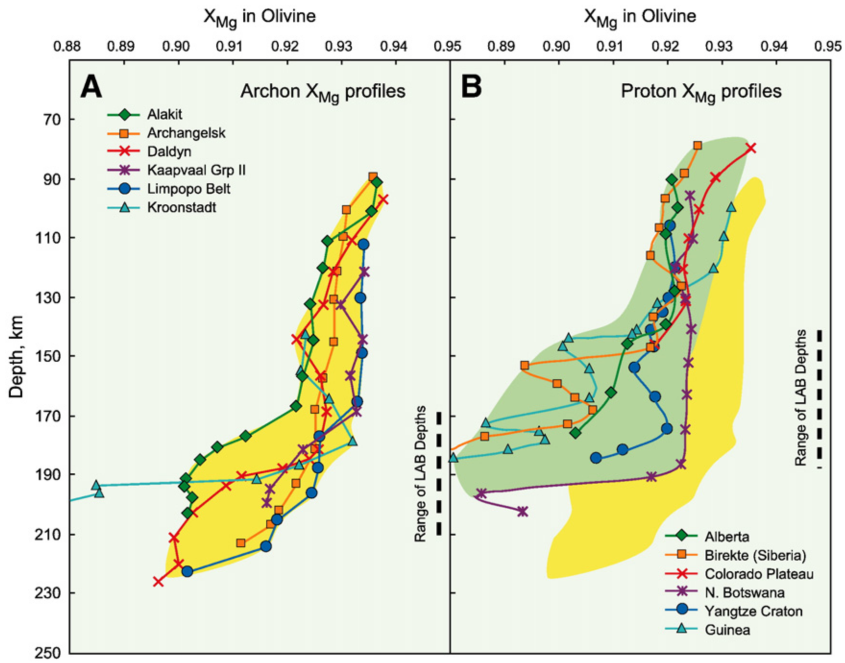

Fig. 5. X_{Mg} vs depth (see Fig. 4) for different lithospheric sections. (A) Archons (cratons unaffected by tectonothermal events <2.5 Ga old); (B) protons (areas affected by tectonothermal events 2.5–1.0 Ga). Dashed bars on right-hand side show the range of LAB depths inferred for these profiles. After O'Reilly and Griffin (2006).

cratonic "LAB" is defined by a zone of melt infiltration, which strongly modifies the composition of pre-existing depleted lithospheric mantle. But what are these melts?

2.4. Eclogites and the LAB

Eclogite is the high-pressure equivalent of basalt (*sensu lato*); it consists of garnet + omphacitic clinopyroxene and may contain a range of minor minerals including phlogopite, coesite, kyanite, rutile, sulfide and diamond. Eclogite lenses are found in many localities where pieces of oceanic or continental crust have been subducted to depths of 20–>200 km and then exhumed. Eclogite xenoliths are rare to common in many kimberlites and other cratonic eruptive rocks. Alkali basalts and related rocks in off-craton settings may carry xenoliths of garnet pyroxenites, representing the shallower equivalent of the eclogite xenoliths found in cratonic settings. These garnet pyroxenites have a similar bulk compositional range to eclogites but have equilibrated in the higher geothermal regimes characteristic of off-craton terranes.

The simple mineral assemblage of eclogites allows the calculation of an equilibration temperature, using any of several calibrations of the Fe–Mg partitioning between gnt and cpx, but they rarely contain other phases such as opx, that would allow a direct calculation of *P*. The usual approach to this problem is to assume a *P* (often 30 or 50 kb). The resulting *T* values for a single xenolith suite may spread over 100–300 °C; this has led to the view that the eclogites are distributed widely through the SCLM, and has been used to support "subduction–stacking" models for the formation of the cratonic SCLM.

However, each of the gnt–cpx thermometers contains a pressure-dependent term, so that solution for *T* at a range of *P* generates a line in *P*–*T* space. If we assume that the eclogites have equilibrated at ambient *T* along the geotherm derived from the peridotite xenoliths (or their garnets) from the same kimberlite, we can project this line to the geotherm and derive a *P* estimate (Griffin and O'Reilly, 2007a). When this is done for a large eclogite suite, such as the well-studied one from the Roberts Victor mine in South Africa (Fig. 7A), we find that rather than being widely distributed, the eclogites are tightly clustered near the base of the depleted SCLM, coincident with the zone of melt-related metasomatism that marks the "LAB".

In the SW part of the Kaapvaal craton, the SCLM has been strongly metasomatised in the interval between the intrusion of the Group II (older than 110 Ma) and Group I (younger than 90 Ma) kimberlites (Bell et al., 2005; Foley, 2008; Kobussen et al., 2008, 2009). A composite chemical tomography section for the Group II (older) kimberlites in this area (Fig. 7B) shows a thick depleted SCLM with a zone of melt-related metasomatism below 190 km, and the abundant eclogites from one of these kimberlites are concentrated between 195 and 215 km. Garnets and xenoliths from Group II peridotites record a geotherm close to a 35 mW/m^2 conductive model (Griffin et al., 1993; Bell et al., 2005). By the time the Group I kimberlites intruded in the same area, the SCLM had been thinned and refertilised, and its geotherm had been raised significantly (40 mW/m^2); melt-related metasomatism is prominent at depths below ca 140 km, and intense below 170 km (Griffin et al., 2003a; Griffin and O'Reilly, 2007b; Kobussen et al., 2008). The eclogites from one of the Group I kimberlites are concentrated around the new, shallower "LAB" at ca 165 km, with a minor population at about 140 km, although there was no evidence of eclogites at this depth in the xenolith population from the older Group II kimberlites in this region. These distributions strongly suggest that the melt-related metasomatism is directly connected with the emplacement of the eclogites, and that this emplacement may have been instrumental in the thinning of the SCLM over a 20-Ma period.

Cratonic eclogites are now commonly regarded as fragments of subducted oceanic slabs (see review by Jacob, 2004), although this interpretation ignores the abundant evidence that many of the eclogites had high-*T* magmatic precursors, mainly aluminous cpx, from which garnet and other phases have exsolved (Lappin, 1978; Smyth and Caporuscio, 1984; Sautter and Harte, 1988). However, there is no tectonic scenario that allows for the shallow subduction of an oceanic slab beneath the Kaapvaal craton in the time interval 110–90 Ma, to coincide with the emplacement of eclogites beneath the thinned SCLM sampled by Group I kimberlites. It therefore seems more likely that these eclogites, and other suites clustered at the "LAB" (Fig. 7A) represent magmas that ponded at the base of the depleted SCLM; their intrusion and crystallization would have supplied both the heat to

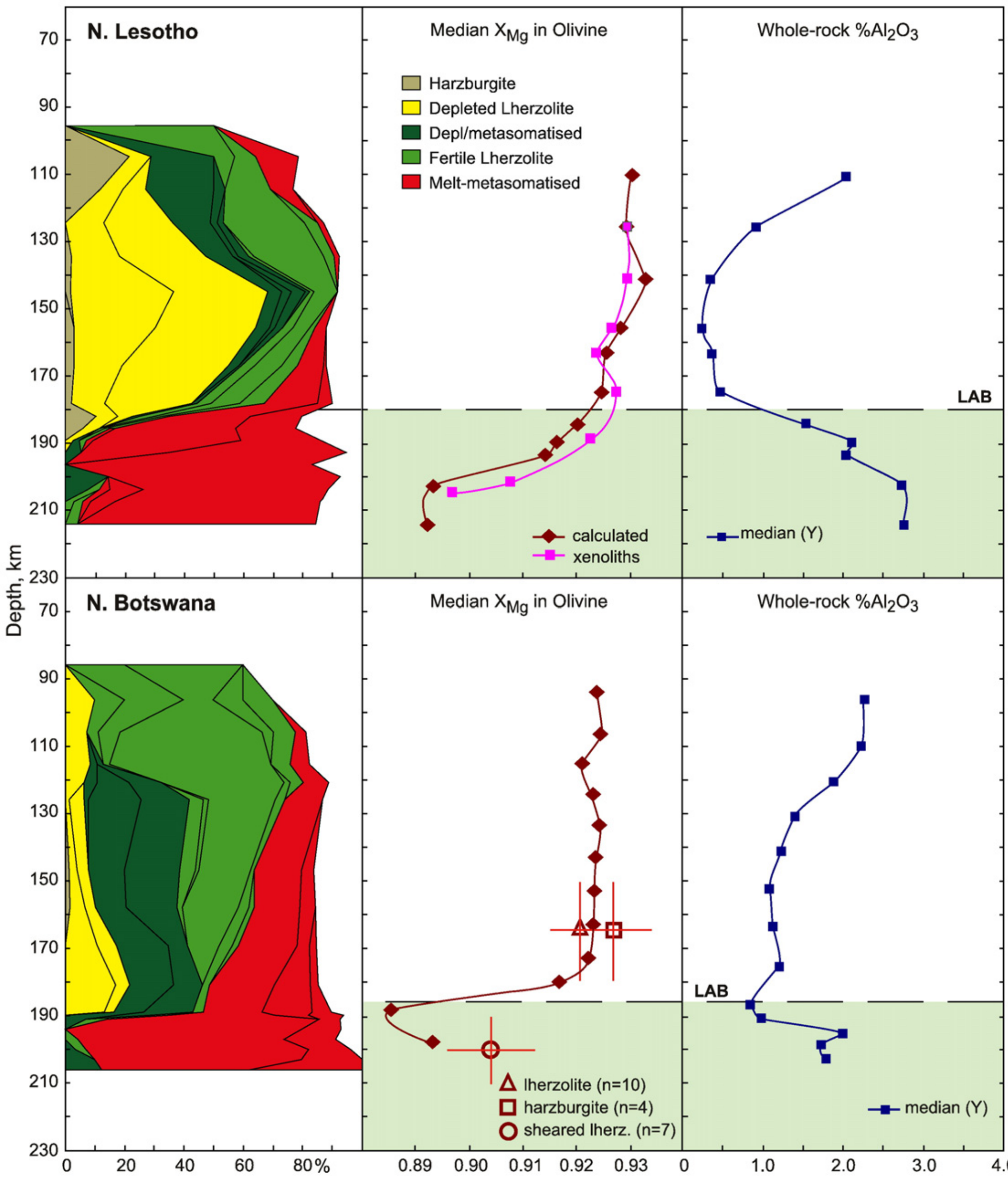

Fig. 6. Chemical tomography sections for Archean SCLM. (A) Northern Lesotho (Cretaceous). (B) Northern Botswana (Cretaceous). After Griffin et al. (2003a).

perturb the geotherm and fluids to produce the metasomatism that marks the "geochemical LAB".

2.5. Is there evidence for other fluid processes at the LAB?

Metasomatic processes recorded in garnet megacrysts and their inferred origin from infiltrating mafic magmas, are consistent with the concept that eclogites preferentially cluster at the LAB, and represent ponding of the mafic magmas due to rheology differences, as discussed above. However, there is evidence that carbonate and/or carbonate-rich fluids are also present in the lowermost lithospheric mantle, and represent another type of infiltrating fluid at that depth. Petrographic evidence is provided, for example, by the carbonate-bearing globules, inferred to represent evolving carbonatitic/kimberlitic fluids trapped in megacrystalline lherzolites derived from about 220 km beneath the Slave Craton (van Achterberg et al., 2004; Araujo et al., 2009). It has been shown experimentally that the LAB beneath cratons is coincident with the depth where the mantle solidus is exceeded for some compositions and is the level where segregation of carbonate-rich fluids can occur (e.g. Wyllie, 1988; Gudfinnsson and Presnall, 1996). Gaillard et al. (2008) demonstrated that carbonate melts are much more highly conductive than silicate melts, and that small degrees of carbonate melt will wet grain boundaries. The presence of both carbonate fluids and mafic melts at this level provides a possible explanation for the magnetotelluric signals that appear to indicate that the LAB may be detected by lower resistivity (Jones et al., 2010-this volume).

2.6. Thickening the SCLM: plume-head accretion?

The discussion above has focused mainly on examples of lithosphere thinning, as melts from below have metasomatised the base of the depleted SCLM. However, the SCLM might also be thickened by the accretion of "plumes", broadly defined as mass upwellings from the deeper levels of the Earth. Kaminsky and Jaupart (2000) have modeled the effects of plume impact on the SCLM. These models predict heating and erosion of the SCLM, followed by large-scale subsidence as the plume head, now accreted to the base of the SCLM, cools; this assumes that the plume head is less depleted than the pre-existing SCLM. This

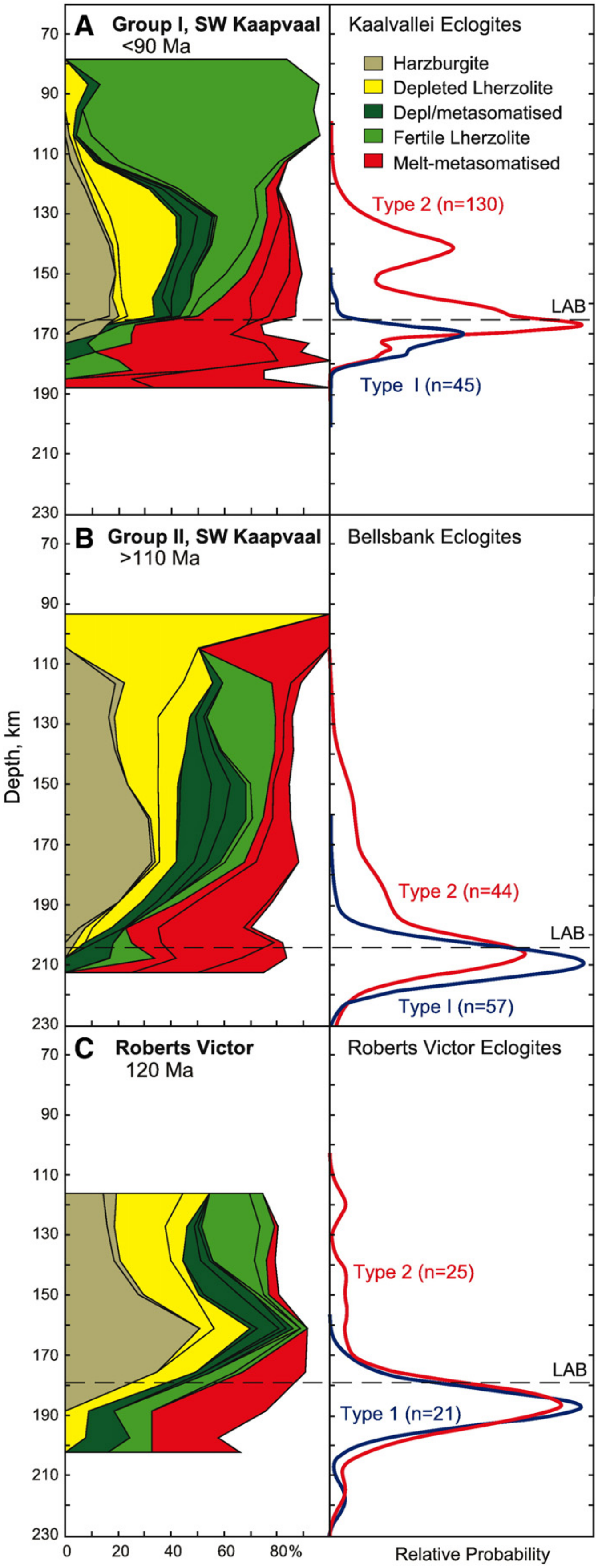

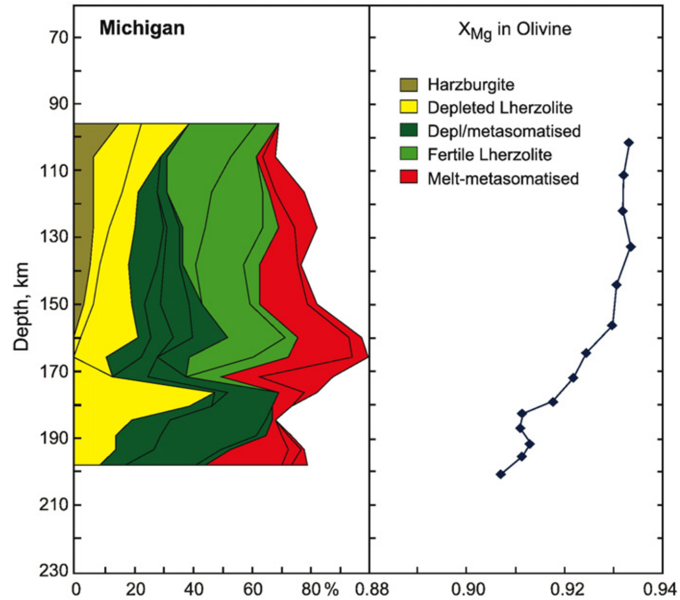

Fig. 8. Chemical tomography section for the northern Michigan Basin, showing a discontinuity at ≈165–175 km. T estimates for eclogite xenoliths from the Michigan kimberlites place them at the depth of the discontinuity. Data from Griffin et al. (2004a).

model was used to explain the development of large subcircular basins in cratonic areas; one example is the Paleozoic Michigan Basin of North America.

The northern edge of the Michigan Basin was intruded by kimberlites shortly after initiation of the basin sedimentation. A chemical tomography section derived from these kimberlites (Fig. 8) offers support for the plume model. The SCLM above 160 km depth is typical of many on the edges of Archean cratons, with both depleted and refertilised rocks. There is a gap of ca 10–15 km (165–180 km) in which there are few peridotitic garnets; T estimates for eclogites from the Michigan kimberlites fall into this gap (950–1100 °C; McGee and Hearn, 1984). Below 180 km, there are moderately depleted lherzolites, and the abundance of more fertile rocks increases rapidly with depth. We suggest that the rocks below 180 km represent the proposed plume head, and the eclogites represent partial-melting products concentrated at the top of the plume; the greater degree of depletion just below 180 km could reflect the extraction of these melts. Similar relationships have been documented beneath the Williston Basin, using garnet data from the Alberta kimberlites that intersect the edges of that basin (Griffin et al., 2004a).

An even more compelling argument for plume accretion can be made for the Slave Craton in northern Canada. A chemical tomography section constructed from xenocrysts and xenoliths in kimberlites in the Lac de Gras area (Fig. 9; Pearson et al., 1999; Griffin et al., 1999a,b; Aulbach et al., 2007) shows an ultradepleted upper layer extending down to a sharp boundary at ca 160 km depth; this is underlain by a mantle section more similar to many from other Archean areas (cf Figs. 5, 6). Eclogites are strongly concentrated around the boundary between the two layers of the SCLM, with a smaller concentration near 200 km, the deepest levels sampled. Re–Os data indicate that the upper layer of the SCLM formed at ≈3.4 Ga (Westerlund et al., 2003), whereas the lower layer formed at ca 3.2 Ga (Aulbach et al., 2004). Studies of inclusions in diamonds from Lac de Gras kimberlites have found an unusually large proportion of minerals from the transition zone and lower mantle (Davies et al., 1999, 2004a,b),

Fig. 7. Distribution of eclogites in representative mantle sections. (A) Eclogite distribution beneath the Kaapvaal craton in Group II time (>120 Ma) and Group I time (≤90 Ma). Refertilisation has moved the "LAB" up by 30–40 km between these two episodes of kimberlite emplacement. (B) Roberts Victor eclogite suite, superposed on Chemical Tomography section derived from peridotitic garnets in the Roberts Victor kimberlite. Data from Griffin and O'Reilly (2007a,b).

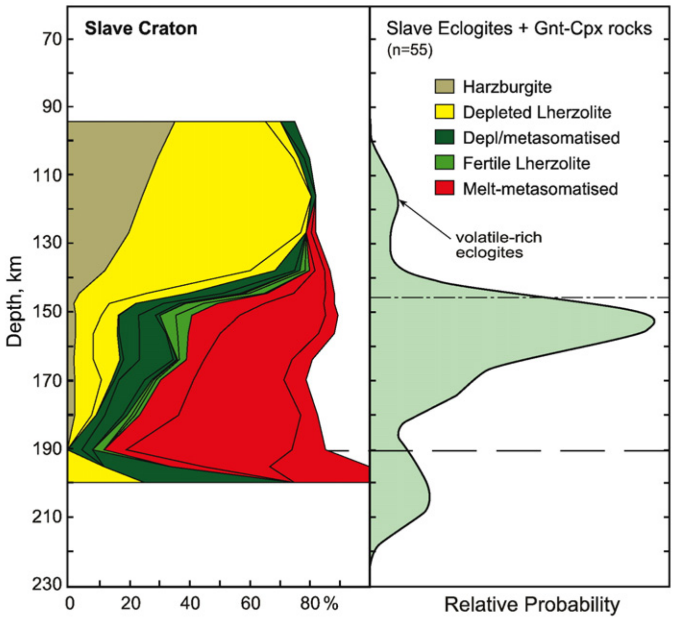

Fig. 9. Chemical tomography section for the central part of the Slave Craton, N. Canada, showing a strongly layered SCLM with an ultradepleted upper part and a more fertile lower part, interpreted as the head of a plume (after Griffin et al., 1999a). Eclogites are concentrated at the base of the ultradepleted layer, and at the base of the section. Pie chart shows proportion of different diamond parageneses; note the high proportion of "super-deep" diamonds from the Transition Zone and lower mantle (Davies et al., 1999, 2004a).

and these diamonds are inferred to be derived from the lower layer of the SCLM, where diamonds are more likely to be stable (Fig. 9). The presence of the "super-deep" diamonds strengthens the interpretation of the two-layered structure as reflecting the ca 3.2 Ga impingement of a plume head on the base of an extremely depleted 3.4 Ga SCLM. The eclogite-rich layer at the junction of the two types of mantle is, as in the Michigan case, consistent with the ponding of magmas rising from the top of the plume.

"Super-deep" diamonds with ferropericlase inclusions were first recognized in the kimberlites of the eastern Gawler craton in S. Australia (Scott-Smith et al., 1984). The chemical tomography section from these kimberlites (Fig. 10) also shows a striking two-layered SCLM (Gaul et al., 2003). This is a feature of all localities (for which we have data) that contain known super-deep diamonds; it may be a signature of plume-head accretion to the SCLM.

2.7. Where is the sub-cratonic asthenosphere? The complication of deep continental roots

The observations summarised above suggest that the "LAB" beneath cratons represents a zone of melt accumulation and metasomatism at the base of the most depleted portion of the SCLM. This buoyant and depleted material may have served as a chemical and rheological barrier, but one that could be broken down by metasomatic activity, so that the LAB can move upwards through time. If the eclogites represent frozen magmas and/or their cumulates, they could be defined as coming from the asthenosphere. But does the asthenosphere lie directly beneath them?

Seismic tomography images show high-velocity "mantle roots" beneath most cratons, possibly corresponding to the "tectosphere" of Jordan (1988); these deep roots require not only low *T*, but depleted compositions (e.g. Deen et al., 2006). Beneath many cratons, these roots extend to depths of ≥300 km and in some regions they may reach the transition zone (e.g. Masters et al., 1996; Ritsema et al., 1999; Mégnin and Romanowicz, 2000; Ritsema and van Heijst, 2000; Godey et al., 2004; Nettles and Dziewonski, 2008; Begg et al., 2009; O'Reilly et al., 2009). Even beneath the Kaapvaal craton, which appears to have a less robust "root" than other African cratons (Begg et al., 2009), detailed tomography (James et al., 2001; Fouch et al., 2004) suggests depths of ≥250 km. These images imply that the chemically-defined "LAB" is not the real base of the cratonic mantle; it may simply represent a zone of melt accumulation and metasomatism within the deeper cratonic root, consistent with the experimental results of Wyllie (1988) and Gudfinnsson and Presnall (1996).

Peridotite xenoliths derived from below this zone of melt accumulation have not been recognized. The only rock samples that clearly are from deeper levels are eclogitic/pyroxenitic xenoliths from Jagersfontein that have inverted from majoritic garnet (Haggerty and Sautter, 1990; Griffin, 2008). These are compositionally similar to inclusions of majoritic garnet and associated phases in diamonds from Monastery Mine (Moore and Gurney, 1985; Moore et al., 1991), Sao Luis (Brazil; Harte et al., 1999; Kaminsky et al., 2001) and a few other occurrences (Davies et al., 1999, 2004a,b). On geophysical grounds, these rock types are unlikely to be major constituents of the deep mantle.

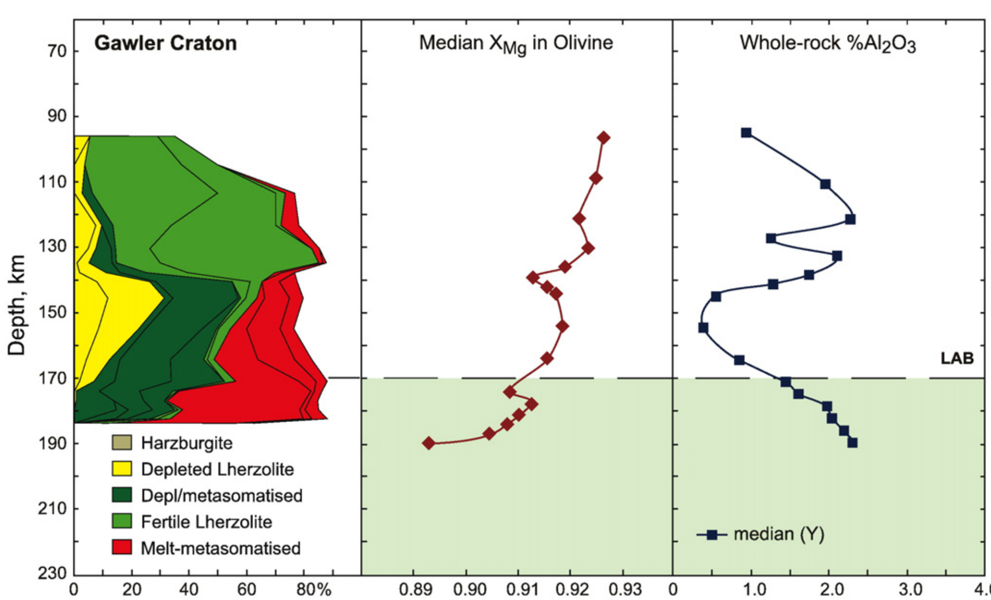

Fig. 10. Chemical tomography section for the SE part of the Gawler Craton, S. Australia, showing two-layered SCLM (Gaul et al., 2003). This is the locality from which "super-deep" diamonds were first recognized (Scott-Smith et al., 1984), and from this we infer that the lower part of the SCLM represents an accreted plume head.

The conclusion must be that we have no xenolithic samples of the "asthenosphere", in the sense of a convecting ultramafic mantle, beneath any of the stable cratonic areas. Indeed, the presence of the deep and irregular roots imaged by seismic tomography (e.g. Begg et al., 2009) raises the question of whether it is relevant to think of a convecting layer under a continent such as Africa, or much of cratonic North America; any convective movement at depths of a few hundred km is likely to be dominated by a vertical component, controlled by the steep sides of the mantle roots (Begg et al., 2009; O'Reilly et al., 2009).

3. Off-craton asthenosphere

The most likely place to sample the asthenosphere may be in extensional zones, where the disruption of the SCLM allows the asthenospheric mantle to well up and underplate the lithosphere, where it can be sampled by basaltic magmas. One example is the North China Craton, where the lithospheric root has been disrupted and largely replaced since Ordovician time (Griffin et al., 1998b; Xu et al., 1998, 2003; Zheng et al., 2005, 2007; Yang et al., 2008). The "new" lithosphere sampled by Tertiary basalts is 50–100 km thick (Chen et al., 2008; Chen, 2010-this volume), and consists of fertile spinel lherzolites, with garnet lherzolites in the deepest layers (>60 km). Beneath the Phanerozoic mobile belts of southeastern Australia, the upper parts of the SCLM consist of spinel lherzolites with low median X_{Mg} but widely variable Al_2O_3 (Fig. 11); some of the depleted lherzolites are relicts of Proterozoic SCLM (Handler et al., 1997; McBride et al., 1996; Powell and O'Reilly, 2007). The deepest xenoliths sampled by Tertiary basalts in this area are rare garnet lherzolites. The Tertiary to Recent basaltic rocks of the Baikal rift zone (Litasov and Taniguchi, 2002) sample an upper spinel–peridotite SCLM with widely variable degrees of depletion, and the deepest samples are fertile garnet lherzolites.

In each of these areas there is a striking contrast between the wide range of depletion seen in the shallower spinel peridotite xenoliths, and the relatively restricted compositional range of the garnet lherzolite xenoliths (Fig. 12). The latter are strikingly similar from area to area. They have a mean composition very similar to estimates of the Primitive Upper Mantle (4–4.5% Al_2O_3, 3.2–3.6% CaO, Mg# 89.3–90; see compilation by Griffin et al., 1999c), $X_{Mg} \approx 0.89$, and modes of 9–10% cpx and 15–20% garnet. Similar rocks are found among the spinel lherzolite xenoliths in young extensional terrains (Fig. 12). Model calculations based on trace-element compositions of the clinopyroxenes suggest that these fertile rocks have undergone less than 2–3% melt extraction (e.g. Xu et al., 2003). We suggest that these fertile rocks, and especially the deeper garnet lherzolites, may represent samples of the asthenosphere, where lithospheric extension or delamination has allowed it to rise up and underplate beneath thinning lithosphere.

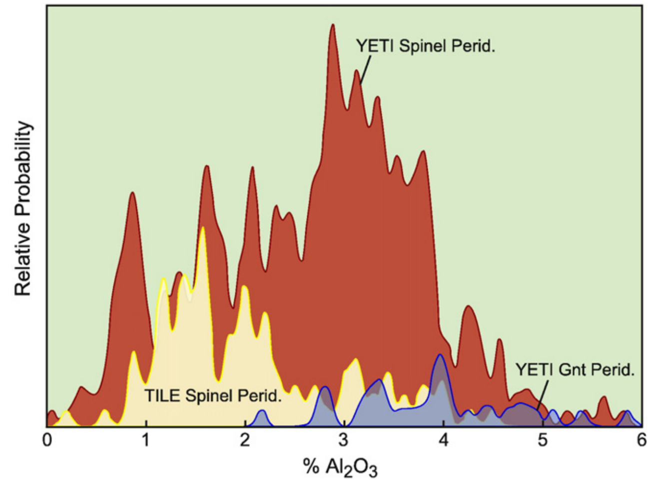

Fig. 12. Cumulative-probability plot of whole-rock Al_2O_3 contents in spinel lherzolite and garnet peridotite xenoliths. YETI suite is from Phanerozoic extensional belts. TILE suite is from areas with Proterozoic to Phanerozoic crust showing little evidence of extension; many TILE samples may represent refertilised Archean SCLM. Data from Griffin et al. (1999b).

4. The LAB — a movable boundary

It should be apparent from this summary that the LAB, at least as geochemically defined, is not a stable feature. Examples cited above (Figs. 8–10) suggest that the LAB has been moved down in some areas

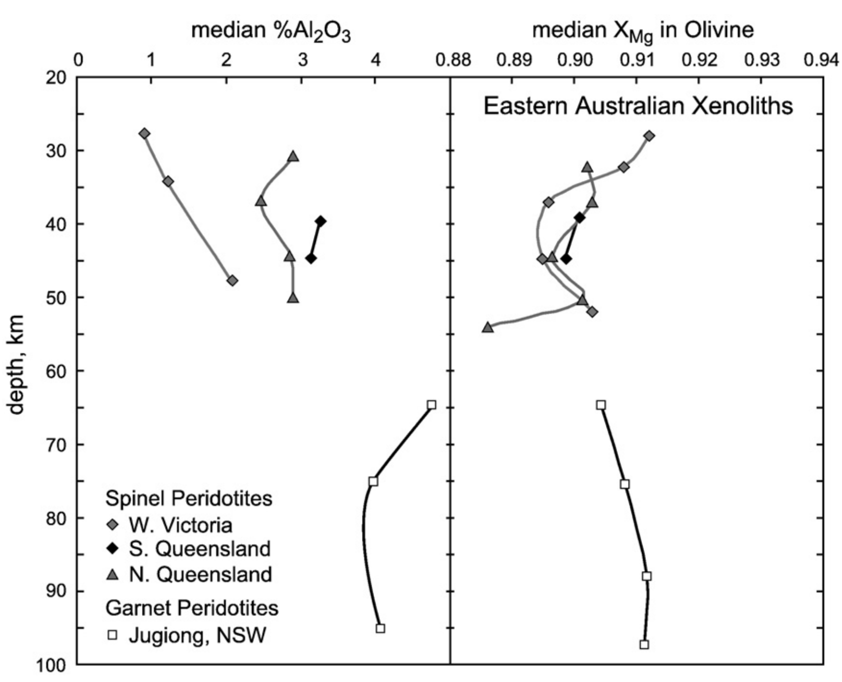

Fig. 11. Variation of whole-rock Al_2O_3 and X_{Mg} in olivine beneath localities in eastern Australia. Data derived from spinel–lherzolite xenoliths to 60 km depth, and from garnet xenocrysts below 60 km.

by the accretion of plume heads to pre-existing SCLM. In these cases, the earlier "LAB" may remain as a marked discontinuity in composition, as in the Slave Province. We have little evidence that this process is operating beneath continents at present, but oceanic plateaus such as Ontong Java and Kerguelen may be useful analogues (Taylor, 2006; Weis and Frey, 1996; Gregoire et al., 1998; Hassler and Shimizu, 1998).

Depleted cratonic SCLM of any thickness is buoyant relative to the convecting asthenosphere (Poudjom Djomani et al., 2001; O'Reilly et al., 2001) and cannot be removed ("delaminated") by gravitational forces. It may be pushed down temporarily by tectonic forces (e.g. continental collision/subduction) but ultimately will rebound, as shown by the exhumation of UHP terranes. However, the base of the depleted SCLM is exposed to ascending magmas, which can cause metasomatism and move the "LAB" upward. This sort of "chemical thinning", accompanied by a rise in the geotherm, occurred beneath southern Africa between 120 and 100 Ma ago, as shown in Fig. 7B; a more sophisticated analysis by Kobussen et al. (2008, 2009) gives a 4D image of the regional distribution of this process. However, as discussed above, the mantle beneath the refertilised zone may still constitute an intact lithospheric root, cooler and somewhat less fertile than the convecting asthenosphere.

This refertilisation process will increase the density of the peridotitic SCLM, and the increase in density would be accentuated by the accumulation of eclogites (cooled melts), which may make up at least 30% of the mantle at the base of the depleted SCLM (Fig. 7; Griffin and O'Reilly, 2007a). This enriched layer might then be susceptible to delamination, producing a real thinning of the SCLM and a shallower "real" LAB. A process of this type may have occurred beneath India during the breakup of Gondwana; 1100 Ma kimberlites in the Dharwar craton sampled a thick root, but seismic data suggest that no root is present in that area today, and this may explain India's rapid northward drift (Griffin et al., 2009b).

These processes are probably enhanced in regions of active extension, when the cratonic SCLM is physically disrupted, allowing the asthenosphere to well up into incipient rifts. The eastern part of the North China Craton is perhaps the most striking example; the Basin and Range Province of western North America may be another, as Re–Os data from spinel peridotite xenoliths in alkali basalts reveal the presence of Archean SCLM remnants beneath the extending crust (Lee et al., 2001).

The SCLM beneath Phanerozoic mobile belts is generally thin, hot and fertile. If the fertile garnet peridotites discussed above represent accreted asthenosphere, they suggest that thin SCLM has been underplated and thickened, moving the LAB to greater depths. However, this situation is likely to be transitory. Once this fertile deep layer cools to a typical Phanerozoic geotherm, it is unstable relative to the asthenosphere (Poudjom Djomani et al., 2001) and can easily delaminate to produce a shallow LAB, which in turn can be underplated by rising asthenosphere, in a cyclic process with no predictable end (Zheng et al., 2006b).

5. Future focus

Although there has been progress over recent years in furthering our understanding of the nature and location of the lithosphere–asthenosphere boundary (as discussed in this contribution and by Jones et al. (2010-this volume)), there are still more questions than hard answers. Recent advances in many areas of the geosciences include geochemical techniques that allow us to identify subtle geochemical fingerprints in lithospheric samples and assess the timing of mantle events; understanding the significance of differences in the compositional signatures of basaltic magmas for asthenospheric evolution and the underlying geodynamic processes; improved resolution of seismic tomography and potential-field data; improved codes for numerical modeling of geodynamic processes in the Earth; better understanding of the significance of deformation mechanisms and anisotropy characteristics of mantle minerals.

Future advances in defining this controversial boundary are critical to our understanding of the geodynamic and geochemical evolution of Earth, and will benefit most from an integrated, interdisciplinary approach encompassing all of these aspects.

Acknowledgments

The ideas presented here have been developed through many discussions with many colleagues over more than a decade, including more recently Graham Begg, Jon Hronsky, Lev Natapov, Craig O'Neill, Steve Grand, David Mainprice, Juan Carlos Afonso, Olivier Alard and participants in Session EIL-03 on "The lithosphere/asthenosphere boundary: Nature, formation and evolution from Hadean to now" at the 33rd International Geological Congress (IGC) in Oslo. We are particularly grateful to Paul Morgan for his contributions to the thermal modeling and for many useful discussions, and to Norman Pearson for his long-term collaboration and support. This work has been supported by ARC and Macquarie University funding to S.Y. O'Reilly and W.L. Griffin, and collaborative research with industry partners. This is contribution #650 from the ARC National Key Centre for Geochemical Evolution and Metallogeny of Continents (www.es.mq.edu.au/GEMOC).

References

Afonso, J.C., Fernandez, M., Ranalli, G., Griffin, W.L., Connolly, J.A.D., 2008. Integrated geophysical–petrological modeling of the lithosphere and sublithospheric upper mantle: methodology and applications. Geochemistry, Geophysics, Geosystems 9, Q05008. doi:10.1029/2007GC001834.

Araujo, D.P., Griffin, W.L., O'Reilly, S.Y., 2009. Mantle melts, metasomatism and diamond formation: Insights from melt inclusions in xenoliths from Diavik, Slave Craton. Lithos 112 (Supp. 2), 675–682.

Aulbach, S., Griffin, W.L., Pearson, N.J., O'Reilly, S.Y., Kivi, K., Doyle, B.J., 2004. Mantle formation and evolution, Slave Craton: constraints from HSE abundances and Re–Os systematics of sulfide inclusions in mantle xenocrysts. Chemical Geology 208, 61–88.

Aulbach, S., Griffin, W.L., Pearson, N.J., O'Reilly, S.Y., Doyle, B.J., 2007. Lithosphere formation in the central Slave Craton (Canada): plume subcretion or lithosphere accretion? Contributions Mineralogy Petrology 154, 409–427.

Begg, G.C., Griffin, W.L., Natapov, L.M., O'Reilly, S.Y., Grand, S.P., O'Neill, C.J., Hronsky, J.M.A., Poudjom Djomani, Y., Swain, C.J., Deen, T., Bowden, P., 2009. The lithospheric architecture of Africa: seismic tomography, mantle petrology and tectonic evolution. Geosphere 5, 23–50.

Bell, D.R., Gregoire, M., Grove, T.L., Chatterjee, N., Carlson, R.W., Buseck, P.R., 2005. Silica and volatile-element metasomatism of Archean mantle: a xenolith-scale example from the Kaapvaal craton. Contributions to Mineralogy and Petrology 152, 335–347.

Boyd, F.R., 1970. Garnet peridotites and the system $CaSiO_3$–$MgSiO_3$–Al_2O_3. Mineralogical Society of America Special Paper 3, 63–75.

Boyd, F.R., 1987. High- and low-temperature garnet peridotite xenoliths and their possible relation to the lithosphere–asthenosphere boundary beneath southern Africa. In: Nixon, P.H. (Ed.), Mantle Xenoliths. Wiley, New York, pp. 403–412.

Boyd, F.R., 1989. Compositional distinction between oceanic and cratonic lithosphere. Earth and Planetary Science Letters 96, 15–26.

Boyd, F.R., Nixon, P.H., 1975. Origins of the ultramafic nodules from some kimberlites of northern Lesotho and the Monastery Mine, South Africa. Physics and Chemistry of the Earth 9, 432–454.

Boyd, F.R., Pearson, D.G., Mertzman, S.A., 1999. Spinel-facies peridotites from the Kaapvaal Root. Proceedings of the 7th International Kimberlite Conference: Cape Town, Red Roof Design, pp. 40–47.

Brey, G.P., Kohler, T., 1990. Geothermobarometry in four-phase lherzolites II. New thermobarometers and practical assessment of existing thermobarometers. Journal of Petrology 31, 1353–1378.

Brey, G.P., Kohler, T., Nickel, K.G., 1990. Geothermobarometry in four-phase lherzolites I. Experimental results from 10 to 60 kb. Journal of Petrology 31, 1313–1352.

Brey, G.P., Bulatov, V.K., Girnis, A.V., 2008. Geobarometry for peridotites: experiments in simple and natural systems from 6 to 10 GPa. Journal of Petrology 49, 3–24. doi:10.1093/petrology/egm067.

Canil, D., 1994. An experimental calibration of the "nickel in garnet" geothermometer with applications. Contributions to Mineralogy and Petrology 117, 410–420.

Canil, D., 1999. The Ni-in-garnet geothermeter: calibration at natural abundances. Contributions to Mineralogy and Petrology 136, 240–246.

Chen, L., 2010. Concordant structural variations from the surface to the base of the upper mantle in the North China craton and its tectonic implication. Lithos 120, 96–115 (this volume).

Chen, L., Wang, T., Zhao, L., Zheng, T.Y., 2008. Distinct lateral variation of lithospheric thickness in the Northeastern North China Craton. Earth and Planetary Science Letters 267, 56–68.

Davies, R., Griffin, W.L., Pearson, N.J., Andrew, A., Doyle, B.J., O'Reilly, S.Y., 1999. Diamonds from the deep: pipe DO-27, Slave Craton, Canada. Proceedings of the 7th International Kimberlite Conference, Red Roof Design, Cape Town, pp. 148–155.

Davies, R.M., Griffin, W.L., O'Reilly, S.Y., Doyle, B.J., 2004a. Mineral inclusions and geochemical characteristics of microdiamonds from the DO27, A154, A21, A418, DO18, DO27 and Ranch Lake kimberlites, Lac de Gras, Slave Craton, Canada. Lithos 77, 39–55.

Davies, R.M., Griffin, W.L., O'Reilly, S.Y., 2004b. Inclusions in diamonds from the K14 and K10 kimberlites, Buffalo Hills, Alberta, Canada: diamond growth in a plume? Lithos 77, 99–111.

Deen, T., Griffin, W.L., Begg, G., O'Reilly, S.Y., Natapov, L.M., 2006. Thermal and compositional structure of the subcontinental lithospheric mantle: derivation from shear-wave seismic tomography. Geochemistry, Geophysics and Geosystems. doi:10.1029/2005GC001164.

Finnerty, A.A., Boyd, F.R., 1987. Thermobarometry for garnet peridotites: basis for the determination of thermal and compositional structure of the upper mantle. In: Nixon, P.H. (Ed.), Mantle Xenoliths. Wiley, New York, pp. 381–402.

Foley, S.F., 2008. Rejuvenation and erosion of the cratonic lithosphere. Nature Geoscience 1, 503–510.

Fouch, M.J., James, D.E., VanDecar, J.C., van der Lee, S., The Kaapvaal Seismic Group, 2004. Mantle seismic structure beneath the Kaapvaal and Zimbabwe Cratons. South African Journal of Geology 107, 33–44.

Franz, L., Brey, G.P., Okrusch, M., 1996. Steady state geotherm, thermal disturbances and tectonic development of the lower lithosphere underneath the Gibeon Kimberlite Province, Namibia. Contributions to Mineralogy and Petrolgy 126, 181–196.

Gaillard, F., Malki, M., Iacono-Marziano, G., Pichavant, M., Scaillet, B., 2008. Carbonatite melts and electrical conductivity in the asthenosphere. Science 322, 1363–1365.

Gaul, O.F., Griffin, W.L., O'Reilly, S.Y., Pearson, N.J., 2000. Mapping olivine composition in the lithospheric mantle. Earth and Planetary Science Letters 182, 223–235.

Gaul, O., O'Reilly, S.Y., Griffin, W.L., 2003. Lithosphere structure and evolution in southeastern Australia. Geological Society of Australia Special Publication 22, 179–196.

Godey, S., Deschamps, F., Trampert, J., Snieder, R., 2004. Thermal and compositional anomalies beneath the North American continent. Journal of Geophysical Research 109, B01308. doi:10.1029/2002JB002263.

Gregoire, M., Cottin, J.Y., Giret, A., Mattielli, N., Weis, D., 1998. The meta-igneous granulite xenoliths from Kerguelen Archipelago: evidence of a continental nucleation in an oceanic setting. Contributions to Mineralogy and Petrology 133, 259–283.

Gregoire, M., Bell, D.R., Le Roux, A.P., 2002. Trace element geochemistry of phlogopite-rich mafic mantle xenoliths: their classification and their relationship to phlogopite-bearing peridotites and kimberlites revisited. Contributions to Mineralogy and Petrology 142, 603–625.

Gregoire, M., Rabinowic,z, M., Janse, A.J.A., 2006. Mantle mush compaction: a key to understand the mechanisms of concentration of kimberlite melts and initiation of swarms of kimberlite dykes. Journal of Petrology 47, 631–646.

Griffin, W.L., 2008. Major transformations reveal Earth's deep secrets. Geology 36, 95–96.

Griffin, W.L., O'Reilly, S.Y., 1987. Is the Moho the crust–mantle boundary? Geology 15, 241–244.

Griffin, W.L., O'Reilly, S.Y., 2007a. Cratonic lithospheric mantle: is anything subducted? Episodes 30, 43–53.

Griffin, W.L., O'Reilly, S.Y., 2007b. The earliest subcontinental mantle. In: Van Kranendonk, M., Smithies, H., Bennett, V. (Eds.), Earth's Oldest Rocks. Elsevier, Amsterdam, pp. 1013–1035.

Griffin, W.L., Wass, S.Y., Hollis, J.D., 1984. Ultramafic xenoliths from Bullenmerri and Gnotuk maars, Victoria, Australia: petrology of a subcontinental crust–mantle transition. Journal of Petrology 25, 53–87.

Griffin, W.L., Ryan, C.G., Cousens, D.C., Sie, S.H., Suter, G.F., 1989. Ni in Cr-pyrope garnets: a new geothermometer. Contributions to Mineralogy and Petrology 103, 199–202.

Griffin, W.L., Sobolev, N.V., Ryan, C.G., Pokhilenko, N.P., Win, T.T., Yefimova, Y., 1993. Trace elements in garnets and chromites: diamond formation in the Siberian lithosphere. Lithos 29, 235–256.

Griffin, W.L., Smith, D., Ryan, C.G., O'Reilly, S.Y., Win, T.T., 1996. Trace element zoning in mantle minerals: metasomatism and thermal events in the upper mantle. Canadian Mineralogist 34, 1179–1193.

Griffin, W.L., O'Reilly, S.Y., Ryan, C.G., Gaul, O., Ionov, D., 1998a. Secular variation in the composition of subcontinental lithospheric mantle. In: Braun, J., Dooley, J.C., Goleby, B.R., van der Hilst, R.D., Klootwijk, C.T. (Eds.), Structure and Evolution of the Australian Continent. : Geodynamics, vol. 26. American Geophysical Union, Washington, D.C., pp. 1–26.

Griffin, W.L., Zhang, A., O'Reilly, S.Y., Ryan, C.G., 1998b. Phanerozoic evolution of the lithosphere beneath the Sino-Korean Craton. In: Flower, M., Chung, S.L., Lo, C.H., Lee, T.Y. (Eds.), Mantle Dynamics and Plate Interactions in East Asia Mantle Dynamics and Plate Interactions in East Asia. : Geodynamics, vol. 27. American Geophysical Union, pp. 107–126.

Griffin, W.L., Doyle, B.J., Ryan, C.G., Pearson, N.J., O'Reilly, S.Y., Davies, R.M., Kivi, K., van Achterbergh, E., Natapov, L.M., 1999a. Layered mantle lithosphere in the Lac de Gras Area, Slave Craton: composition, structure and origin. Journal of Petrology 40, 705–727.

Griffin, W.L., O'Reilly, S.Y., Ryan, C.G., 1999b. The composition and origin of subcontinental lithospheric mantle. In: Fei, Y., Bertka, C.M., Mysen, B.O. (Eds.), Mantle Petrology: Field Observations and High-pressure Experimentation: A Tribute to Francis R. (Joe) Boyd, Geochemical Society Special Publication No. 6. The Geochemical Society, Houston, pp. 13–45.

Griffin, W.L., Doyle, B.J., Ryan, C.G., Pearson, N.J., O'Reilly, S.Y., Natapov, L., Kivi, K., Kretschmar, U., Ward, J., 1999c. Lithosphere structure and mantle terranes: Slave Craton, Canada. Proceedings of the 7th International Kimberlite Conference. Red Roof Design, Cape Town, pp. 299–306.

Griffin, W.L., O'Reilly, S.Y., Natapov, L.M., Ryan, C.G., 2003a. The evolution of lithospheric mantle beneath the Kalahari Craton and its margins. Lithos 71, 215–241.

Griffin, W.L., O'Reilly, S.Y., Abe, N., Aulbach, S., Davies, R.M., Pearson, N.J., Doyle, B.J., Kivi, K., 2003b. The origin and evolution of Archean lithospheric mantle. Precambrian Research 127, 19–41.

Griffin, W.L., O'Reilly, S.Y., Doyle, B.J., Pearson, N.J., Coopersmith, H., Kivi, K., Malkovets, V., Pokhilenko, N.V., 2004a. Lithosphere mapping beneath the North American Plate. Lithos 77, 873–902.

Griffin, W.L., Graham, S., O'Reilly, S.Y., Pearson, N.J., 2004b. Lithosphere evolution beneath the Kaapvaal craton. Re–Os systematics of sulfides in mantle-derived peridotites. Chemical Geology 208, 89–118.

Griffin, W.L., O'Reilly, S.Y., Afonso, J.C., Begg, G., 2009a. The composition and evolution of lithospheric mantle: a re-evaluation and its tectonic implications. Journal of Petrology 50, 1185–1204.

Griffin, W.L., Kobussen, A.F., Babu, E.V.S.S.K., O'Reilly, S.Y., Norris, R., Sengupta, P., 2009b. A translithospheric suture in the vanished 1-Ga lithospheric root of South India: evidence from contrasting lithosphere sections in the Dharwar Craton. Lithos 112 (Supp. 2), 1109–1119.

Gudfinnsson, G.H., Presnall, D.C., 1996. Melting relations of model lherzolite in the system CaO–MgO–Al_2O_3–SiO_2 at 2.4–3.4 GPa and the generation of komatiites. Journal of Geophysical Research 101 (B12), 27701–27709.

Haggerty, S.E., Sautter, V., 1990. Ultradeep (greater than 300 kilometers), ultramafic upper mantle xenoliths. Science 248, 993–996.

Handler, M.R., Bennett, V.C., Esat, T.M., 1997. The persistence of off-cratonic lithospheric mantle: Os isotopic systematics of variably metasomatised southeast Australian xenoliths. Earth and Planetary Science Letters 151, 61–75.

Harte, B., Freer, R., 1982. Diffusion data and their bearing on the interpretation of mantle nodules and the evolution of the mantle lihtosohere. Terra Cognita 2, 273–275.

Harte, B., Harris, J.W., Hutchinson, M.T., Watt, G.R., Wilding, M.C., 1999. Lower mantle mineral associations preserved in diamond. In: Fei, Y., Bertka, C.M., Mysen, B.O. (Eds.), Mantle Petrology: Field Observations and High-pressure Experimentation: A Tribute to Francis R. (Joe) Boyd, Geochemical Society Special Publication No. 6. The Geochemical Society, Houston, pp. 125–153.

Hassler, D.R., Shimizu, N., 1998. Osmium isotopoic evidence for ancient subcontinental mantle beneath the Kerguelen Islands, southern Indian Ocean. Science 280, 418–421.

Helmstedt, H.H., Gurney, J.J., 1995. Geotectonic controls of primary diamond deposits: implications for area selection. Journal of Geochemical Exploration 53, 125–144.

Jacob, D.E., 2004. Nature and origin of eclogite xenoliths in kimberlites. Lithos 77, 295–316.

James, D.E., Fouch, M.J., VanDecar, J.C., van der Lee, S., Kaapvaal Seismic Group, 2001. Tectospheric structure beneath southern Africa. Geophysical Research Letters 28, 2485–2488.

Jones, A.P., Smith, J.V., Dawson, J.B., 1983. Glasses in mantle xenoliths from Olmani, Tanzania. Journal of Geology 91, 167–178.

Jones, A.G., Plomerova, J., Korja, T., Sodoudi, F., Spakman, W., 2010. Europe from the bottom up: A statistical examination of the central and northern European lithosphere-asthenosphere boundary from comparing seismological and electromagnetic observations. Lithos 120, 14–29 (this volume).

Jordan, T.H., 1988. Structure and formation of the continental tectosphere. Journal of Petrology 29, 11–38 Special Lithosphere Issue.

Kaminsky, E., Jaupart, C., 2000. Lithosphere structure beneath the Phanerozoic intracratonic basins of North America. Earth and Planetary Science Letters 178, 139–149.

Kaminsky, F.V., Zakharchenko, O.D., Davies, R., Griffin, W.L., Kharchatryan-Blinova, G.K., Shiryaev, A.A., 2001. Superdeep diamonds from the Juina area, Mato Grosso State, Brazil. Contributions to Mineralogy and Petrology 140, 734–753.

Kobussen, A.F., Griffin, W.L., O'Reilly, S.Y., Shee, S.R., 2008. The ghosts of lithospheres past: imaging an evolving lithospheric mantle in southern Africa. Geology 36, 515–518.

Kobussen, A.F., Griffin, W.L., O'Reilly, S.Y., 2009. Cretaceous thermo-chemical modification of the Kaapvaal cratonic lithosphere, South Africa. Lithos 1212 (Supp. 2), 886–895.

Kohler, T., Brey, G.P., 1990. Calcium exchange between olivine and clinopyroxene calibrated as a geothermobarometer for natural peridotites from 2 to 60 kb with applications. Geochimica et Cosmochimica Acta 54, 2375–2388.

Lappin, M., 1978. The evolution of a grospydite from the Roberts Victor Mine, South Africa. Contributions to Mineralogy and Petrology 66, 229–241.

Lee, C.-T., Yin, Q., Rudnick, R.L., Jacobsen, S.B., 2001. Preservation of ancient and fertile lithospheric mantle beneath the southwestern United States. Nature 411, 69–73.

Litasov, K.D., Taniguchi, H., 2002. Mantle evolution beneath the Baikal Rift. Center for Northeast Asian Studies. : CNEAS Monograph Series No. 5. Tohoku University, Japan.

MacGregor, I.D., 1974. The system MgO–Al_2O_3–SiO_2: solubility of Al_2O_3 in enstatite for spinel and garnet peridotite compositions. American Mineralogist 59, 110–119.

Masters, G., Johnson, S., Laske, G., Bolton, B.A., 1996. Shear-velocity model of the mantle. Philosophical Transactions of the Royal Society of London A 354, 1385–1411.

McBride, J.S., Lambert, D.D., Greig, A., Nicholls, I.A., 1996. Multistage evolution of Australian subcontinental mantle: Re–Os isotopic constraints from Victorian mantle xenoliths. Geology 24, 631–634.

McGee, E.S., Hearn, B.C., 1984. The Lake Ellen kimberlite, Michigan, USA. In: Kornprobst, J. (Ed.), Kimberlites: I Kimberlites and Related Rocks. Elsevier, Amsterdam, pp. 143–154.

McKenzie, D., Bickle, M.J., 1988. The volume and composition of melt generated by extension of the lithosphere. Journal of Petrology 29, 625–679.

Mégnin, C., Romanowicz, B., 2000. A comparison between tomographic and geodynamic models of the earth's mantle. History and Dynamics of Plate Motions: AGU Geophysical Monograph Series, vol. 121, pp. 257–276.

Mercier, J.-C.C., 1979. Peridotites, xenoliths and the dynamics of kimberlite intrusion. In: Boyd, F.R., Meyer, H.O.A. (Eds.), The Mantle Sample: Inclusions in Kimberlites and other Volcanics. American Geophysical Union, Washington, pp. 197–212.

Moore, R.O., Gurney, J.J., 1985. Pyroxene solid solution in garnets included in diamond. Nature 318, 553–555.

Moore, R.O., Gurney, J.J., Griffin, W.L., Shimizu, N., 1991. Ultra-high pressure garnet inclusions in Monastery diamonds: trace element abundance patterns and conditions of origin. European Journal Mineralogy 3, 213–230.

Nettles, M., Dziewonski, A.M., 2008. Radially anisotropic shear velocity structure of the upper mantle globally and beneath North America. Journal of Geophysical Research 113, B02303. doi:10.1029/2006JB004819.

O'Reilly, S.Y., 1989. Nature of the east-Australian lithosphere. In: Johnson, R.W. (Ed.), Intraplate Volcanism in Eastern Australia and New Zealand. Cambridge University Press, pp. 290–297.

O'Reilly, S.Y., Griffin, W.L., 1985. A xenolith-derived geotherm for southeastern Australia and its geophysical implications. Tectonophysics 111, 41–63.

O'Reilly, S.Y., Griffin, W.L., 1996. 4-D lithospheric mapping: a review of the methodology with examples. Tectonophysics 262, 3–18.

O'Reilly, S.Y., Griffin, W.L., 2006. Imaging chemical and thermal heterogeneity in the sub-continental lithospheric mantle with garnets and xenoliths: geophysical implications. Tectonophysics 416, 289–309.

O'Reilly, S.Y., Griffin, W.L., Stabel, A., 1988. Evolution of Phanerozoic Australian lithoshere: isotopic evidence for magmatic and tectonic underplating. Journal of Petrology Special 1988, 89–108.

O'Reilly, S.Y., Griffin, W.L., Poudjom Djomani, Y., Morgan, P., 2001. Are lithospheres forever? Tracking changes in subcontinental lithspheric mantle through time. GSA Today 11, 4–9.

O'Reilly, S.Y., Zhang, M., Griffin, W.L., Begg, G., Hronsky, J., 2009. Ultradeep continental roots and their oceanic remnants: a solution to the geochemical "mantle reservoir" problem? Lithos 112S, 638–647.

Pearson, D.G., Wittig, N., 2008. Formation of Archaean continental lithosphere and its diamonds: the root of the problem. Journal of the Geological Society London 165, 895–914.

Pearson, D.G., Carlson, R.W., Shirey, S.B., Boyd, F.R., Nixon, P.H., 1995. Stablisation of Archean lithospheric mantle: a Re–Os isotope study of peridotite xenoliths from the Kaapvaal craton. Earth and Planetary Science Letters 134, 341–357.

Pearson, N.J., Griffin, W.L., Doyle, B.J., O'Reilly, S.Y., van Achterbergh, E., Kivi, K., 1999. Xenoliths from kimberlite pipes of the Lac de Gras area, Slave Craton, Canada. Proc. 7th International Kimberlite Conference. Red Roof Design, Cape Town, pp. 644–658.

Pollack, H.N., Chapman, D.S., 1977. On the regional variation of heat flow, geotherms and lithosphere thickness. Tectonophysics 38, 279–296.

Poudjom Djomani, Y.H., O'Reilly, S.Y., Griffin, W.L., Morgan, P., 2001. The density structure of subcontinental lithosphere through time. Earth and Planetary Science Letters 184, 605–621.

Powell, W., O'Reilly, S.Y., 2007. Sulfide mobility in mantle fluids beneath eastern Australia: implications for metasomatic processes and mantle Re–Os chronology. Lithos 94, 132–147.

Ritsema, J., van Heijst, H., 2000. New seismic model of the upper mantle beneath Africa. Geology 28, 63–66.

Ritsema, J., van Heijst, H.J., Woodhouse, J.H., 1999. Complex shear wave velocity structure imaged beneath Africa and Iceland. Science 286, 1925–1928.

Ryan, C.G., Griffin, W.L., Pearson, N.J., 1996. Garnet geotherms: a technique for derivation of P–T data from Cr-pyrope garnets. Journal of Geophysical Research 101, 5611–5625.

Sautter, V., Harte, B., 1988. Diffusion gradients in an eclogite xenolith from the Roberts Victor kimberlite pipe: 1. Mechanism and evolution of garnet exsolution in Al_2O_3-rich clinopyroxene. Journal of Petrology 29, 1325–1352.

Scott-Smith, B.H., Danchin, R.W., Harris, J.W., Stracke, J.K., 1984. Kimberlites near Orroroo, South Australia. In: Kornprobst, J. (Ed.), Kimberlites and Related Rocks. Elsevier, Amsterdam, pp. 121–142. 1984.

Smith, D., Boyd, F.R., 1987. Compositional heterogeneities in a high-temperature lherzolite nodule and implications for mantle processes. In: Nixon, P.H. (Ed.), Mantle Xenoliths. Wiley, New York, pp. 551–562.

Smith, D., Griffin, W.L., Ryan, C.G., Cousens, D.R., Sie, S.H., Suter, G.F., 1991. Trace-element zoning of garnets from The Thumb: a guide to mantle processes. Contributions to Mineralogy and Petrology 107, 60–79.

Smith, D., Griffin, W.L., Ryan, C.G., 1993. Compositional evolution of high-temperature sheared lherzolite PHN1611. Geochimica et Cosmochimica Acta 57, 605–613.

Smyth, J.R., Caporuscio, F.A., 1984. Petrology of a suite of eclogite inclusions from the Bobbejaan kimberlite, II. Primary phase compositions and origin. In: Kornprobst, J. (Ed.), Kimberlites II. The Mantle and Crust–mantle Relationships. Elsevier, Amsterdam, pp. 121–132.

Taylor, B., 2006. The single largest oceanic plateau: Ontong Java–Manihiki–Hikurangi. Earth and Planetary Science Letters 241, 372–380.

Van Achterbergh, E., Griffin, W.L., O'Reilly, S.Y., Ryan, C.G., Pearson, N.J., Kivi, K., Doyle, B.J., 2004. Melt inclusions from the deep Slave lithosphere: implications for the origin and evolution of mantle-derived carbonatite and kimberlite. Lithos 76, 461–474.

Walker, R.J., Carlson, R.W., Shirey, S.B., Boyd, F.R., 1989. Os, Sr, Nd and Pb isotopic systematics of southern African peridotite xenoliths: implications for the chemical evolution of subcontinental mantle. Geochimica et Cosmochimica Acta 53, 1583–1595.

Weis, D., Frey, F.A., 1996. Role of the Kerguelen Plume in generating the eastern Indian Ocean seafloor. Journal of Geophysical Research 101, 13831–13849.

Westerlund, K.J., Shirey, S.B., Richardson, S.H., Gurney, J.J., Harris, J.W., 2003. Re–Os isotope systematics of peridotitic diamond inclusion sulfides from the Panda kimberlite, Slave Craton. Abstract, 8th International Kimberlite Conference, Victoria, B.C., Canada.

Wood, B.J., Banno, S., 1973. Garnet–orthopyroxene and orthopryoxene relationships in simple and complex systems. Contributions to Mineralogy and Petrology 42, 109–124.

Wyllie, P.J., 1988. The origin of kimberlite. Journal of Geophysical Research 85, 6902–6910.

Xu, X., O'Reilly, S.Y., Griffin, W.L., Zhou, X., Huang, X., 1998. The nature of the Cenozoic lithosphere at Nushan, eastern China. In: Flower, M., Chung, S.L., Lo, C.H., Lee, T.Y. (Eds.), Mantle Dynamics and Plate Interactions in East Asia Mantle Dynamics and Plate Interactions in East Asia. : Geodynamics, vol. 27. American Geophysical Union, pp. 167–196.

Xu, S., O'Reilly, S.Y., Griffin, W.L., Zhou, X., 2003. Enrichment of upper mantle peridotite: petrological, trace element and isotopic evidence in xenoliths from SE China. Chemical Geology 198, 163–188.

Yang, J.-H., Wu, F.-Y., Wilde, S.A., Belousova, E.A., Griffin, W.L., 2008. Mesozoic decratonization of the North China Block. Geology 36, 467–470.

Zheng, J., Griffin, W.L., O'Reilly, S.Y., Liou, J.G., Zhang, R.Y., Lu, F., 2005. Late Mesozoic–Eocene mantle replacement beneath the eastern North China Craton: evidence from the Paleozoic and Cenozoic peridotite xenoliths. International Geology Review 47, 457–472.

Zheng, J., Griffin, W.L., O'Reilly, S.Y., Yang, J.S., Zhang, R.Y., 2006a. A refractory mantle protolith in younger continental crust, east-central China: age and composition of zircon in the Sulu UHP peridotite. Geology 34, 705–708.

Zheng, J.P., Griffin, W.L., O'Reilly, S.Y., Zhang, M., Pearson, N.J., Luo, Z., 2006b. The lithospheric mantle beneath the southwestern Tianshan area, NW China. Contributions to Mineralogy and Petrology 151, 457–479.

Zheng, J.P., Griffin, W.L., O'Reilly, S.Y., Yu, C., Zhang, H.F., Pearson, N.J., Zhang, M., 2007. Mechanism and timing of lithospheric modification and replacement beneath the eastern North China Craton: peridotitic xenoliths from the 100 Ma Fuxin basalts and a regional synthesis. Geochimica Cosmochimica Acta 71, 5203–5225.